13th International Symposium on Particle Image Velocimetry – ISPIV 2019
Munich, Germany, July 22-24, 2019

Spectral decomposition of the root-mean-square error for pressure estimation from particle image velocimetry

Roeland de Kat

University of Southampton, Aeronautics and Astronautics, Southampton, UK

r.de-kat@soton.ac.uk

Abstract

Accurate pressure estimates are important for various fluid engineering applications. We can now estimate pressure from particle image velocimetry (PIV), but to make these estimates really useful, we need to identify and quantify error sources. Here we lay the mathematical foundation to decompose the root-mean-square error of the estimate of pressure from PIV in its spectral constituents and show their application to experimental estimates against reference signals. The error power spectrum is the result of both amplitude and phase errors, where the phase errors are correctly captured in the co-spectrum, whereas the modulus of coherency or the coherence disregard phase errors and therefore overestimate the quality of an estimate. Dominant contributing frequencies can be the best described frequencies. Frequency specific errors are defined and their potential application to estimate errors for signals where a reference is unfeasible are discussed.

1 Introduction

Over the last decade, pressure estimation from particle image velocimetry has risen to become a useful tool to extract more information out of velocity measurement such as particle image velocimetry (PIV), see eg Liu and Katz (2006); de Kat and van Oudheusden (2012); van Oudheusden (2013); van Gent et al. (2017). For these techniques to be useful, one needs to know the accuracy of them. A standard measure for accuracy is the likely difference one will encounter between an estimate and the reference signal. Typically this is expressed as a root-mean-square-error (RMSe). Van der Kindere et al. (2019) showed that the RMSe for pressure fluctuations is related to the standard deviations of the estimated signal and the standard deviation of the reference signal (akin to amplitude response) and the crosscorrelation between them (temporal variation match, linked to phase response), see equation 1:

$$\frac{\sigma_{err}}{\sigma_{ref}} = \sqrt{1 + \frac{\sigma_{est}}{\sigma_{ref}} \left(\frac{\sigma_{est}}{\sigma_{ref}} - 2\rho_{est,ref} \right)}. \tag{1}$$

Van der Kindere et al. (2019) and the studies they used for comparison (ie de Kat and van Oudheusden, 2012; Schneiders et al., 2016), see figure 1 show that the RMSe are significant compared to the standard deviation of the reference signal, indicating that more work is needed for accurate (instantaneous) pressure estimates from PIV. RMSe is a blanket statistical measure to indicate the difference between the estimate and the reference for any one point in a time-series. However, it does not indicate what range of frequencies contribute to that error nor what range of frequencies can be accurately estimated, an important quality for a measurement technique (see eg de Kat and van Oudheusden, 2012; McClure and Yarusevych, 2017).

Therefore, to identify what frequencies contribute to the overall error in the signal and to identify the range of frequencies that can be accurately estimated, we will explore the use of a cross-spectral approach to decompose the RMSe into the contributions of different frequencies. For each frequency we will look at how it contributes to the over all error and their individual the amplitude response and the phase match.

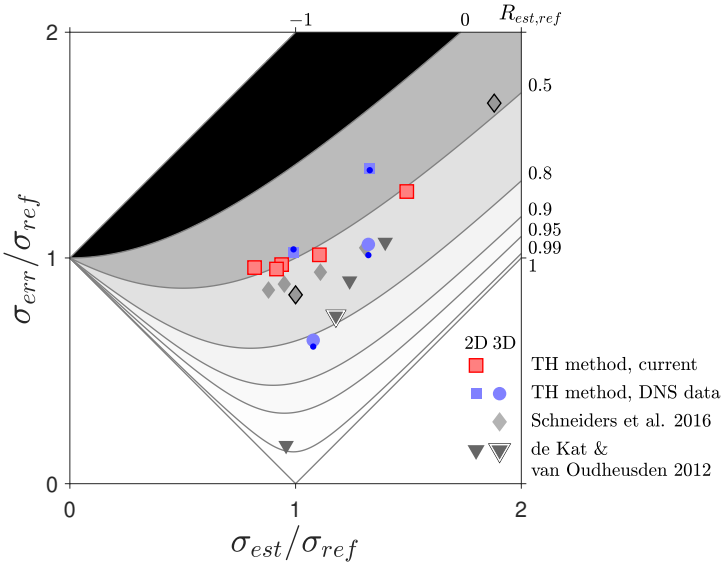

Figure 1: RMSe for pressure from PIV (Van der Kindere et al., 2019). RMSe is a function of the ratio of the standard deviations and the correlation between an estimate and a reference signal. Application to pressure from PIV data shows that despite good agreement in the ratio of standard deviations between estimate and reference, the crosscorrelation needs to significantly improve to reduce the RMSe.

2 Going Spectral

To start off, we will first need to lay the foundation for going spectral. Therefore, we start with some definitions. As is common in spectral analysis we are only considering fluctuations around a zero mean, ie we have decomposed a signal into a mean and fluctuating component and removed the mean.

First, we start with the one-dimensional Fourier transform pair of signal f to obtain its spectrum F:

$$F(\omega) = \frac{1}{\sqrt{2\pi}} \int f(t) e^{-i\omega t} dt \quad ; \qquad f(t) = \frac{1}{\sqrt{2\pi}} \int F(\omega) e^{i\omega t} dt. \tag{2}$$

Note that all integrals without bounds in the current study are over all $\mathbb{R}$ (ie we work with two-sided spectra). From the spectrum, F, the power spectrum, Φ_{ff}, of a single signal f can be determined. Likewise, from the spectra F and G, the cross-power spectrum, Φ_{fg}, of two different signals f and g can be determined:

$$\Phi_{ff}(\omega) = F(\omega)^* F(\omega) \quad ; \qquad \Phi_{fg}(\omega) = F(\omega)^* G(\omega). \tag{3}$$

Where F^* is the complex conjugate of F. Note that the cross-power spectrum, Φ_{fg}, is complex valued, and can be decomposed in the real-valued co-spectrum C_{fg} and quadrature spectrum Q_{fg} (the latter is also known as the phase spectrum):

$$\Phi_{fg}(\omega) = C_{fg}(\omega) + iQ_{fg}(\omega). \tag{4}$$

where the co-spectrum is symmetric and the quadrature spectrum asymmetric.

Second, we define the auto- and cross-correlation for the signals as the expected value (E[·]) of their product (the covariance between the signals at a certain shift, s) and their coefficient forms:

$$R_{ff}(s) = \mathrm{E}[f(t)f(t+s)] \quad ; \qquad R_{fg}(s) = \mathrm{E}[f(t)g(t+s)] \quad ; \tag{5}$$

$$\rho_{ff}(s) = \frac{R_{ff}(s)}{\sigma_f^2} \quad ; \qquad \rho_{fg}(s) = \frac{R_{fg}(s)}{\sigma_f \sigma_g} \tag{6}$$

Comparing these correlations with the power spectra and switching the order of integration results in the following Fourier transform pairs (see also Bendat and Piersol, 2010):

$$\Phi_{ff}(\omega) = \int R_{ff}(s)e^{-i\omega s}ds \quad ; \qquad R_{ff}(s) = \int \Phi_{ff}(\omega)e^{i\omega s}d\omega \quad ; \tag{7}$$

$$\Phi_{fg}(\omega) = \int R_{fg}(s)e^{-i\omega s}ds \quad ; \qquad R_{fg}(s) = \int \Phi_{fg}(\omega)e^{i\omega s}d\omega. \tag{8}$$

Now we can define the coherency of a signal, which is the cross-power spectrum normalised with the square-root of the power spectra (see eg Croux et al., 2001):

$$\mathcal{C}_{fg} = \frac{\Phi_{fg}(\omega)}{\sqrt{\Phi_{ff}(\omega)\Phi_{gg}(\omega)}} = \frac{C_{fg}(\omega) + iQ_{fg}(\omega)}{\sqrt{\Phi_{ff}(\omega)\Phi_{gg}(\omega)}}, \tag{9}$$

which is a complex valued measure with a modulus between zero and one. Coherence, also called squared-coherency or magnitude-squared coherence (see Croux et al., 2001; Bendat and Piersol, 2010), is defined as follows:

$$|\mathcal{C}_{fg}|^2 = \frac{|\Phi_{fg}(\omega)|^2}{\Phi_{ff}(\omega)\Phi_{gg}(\omega)} = \frac{C_{fg}^2(\omega) + Q_{fg}^2(\omega)}{\Phi_{ff}(\omega)\Phi_{gg}(\omega)}, \tag{10}$$

and can be used to quantify how well an input might be used to predict an output (Bendat and Piersol, 2010).

Finally, we will introduce a frequency specific correlation coefficient (also called dynamic correlation Croux et al., 2001) – the spectral equivalent of the cross-correlation – as the co-spectrum normalised by the square-root of the product of the signals' power spectra:

$$\mathcal{R}_{fg}(\omega) = \frac{C_{fg}(\omega)}{\sqrt{\Phi_{ff}(\omega)\Phi_{gg}(\omega)}}, \tag{11}$$

3 Spectral Decomposition of the Error

Now that we have the spectral machinery in place we can start decomposition of the RMSe into its frequency components: $\mathcal{E}(\omega)$. The variance of the error is its correlation value for a zero shift, which can be split into the estimate, reference and cross-correlation values for a zero shift:

$$\sigma_{err}^2 \equiv R_{err,err}(0) = R_{est,est}(0) - 2R_{est,ref}(0) + R_{ref,ref}(0), \tag{12}$$

Using the power spectra Fourier transform pairs defined before, we obtain:

$$\int \mathcal{E}^2(\omega)d\omega = \int \Phi_{est,est}(\omega)d\omega - 2\int \Phi_{est,ref}(\omega)d\omega + \int \Phi_{ref,ref}(\omega)d\omega. \tag{13}$$

and since only the real part of the cross-power spectrum is symmetric and contributes to the second term in the RHS, we find that the error power spectrum can be decomposed into the power spectra and co-spectrum or the estimate and reference signals as follows:

$$\mathcal{E}^2(\omega) = \Phi_{est,est}(\omega) - 2C_{est,ref}(\omega) + \Phi_{ref,ref}(\omega). \tag{14}$$

Now there are two ways we can look at the error power spectrum. First, we will identify which frequencies contribute most to the error and second, we will look at the frequency specific quality of the estimate.

Fractional contributions to total error The fractional contributions of a frequency range to the total error can be determined by dividing the error power spectrum by the variance of the error:

$$\frac{1}{\sigma_{err}^2}\int_{\omega-\Delta\omega}^{\omega+\Delta\omega} \mathcal{E}^2(\omega)d\omega = \frac{1}{\int \mathcal{E}^2(\bar{\omega})d\bar{\omega}}\int_{\omega-\Delta\omega}^{\omega+\Delta\omega} \mathcal{E}^2(\omega)d\omega = \int_{\omega-\Delta\omega}^{\omega+\Delta\omega} \frac{\mathcal{E}^2(\omega)}{\int \mathcal{E}^2(\bar{\omega})d\bar{\omega}}d\omega. \tag{15}$$

Or it can be referenced against the reference signal:

$$\frac{1}{\sigma_{ref}^2}\int_{\omega-\Delta\omega}^{\omega+\Delta\omega} \mathcal{E}^2(\omega)d\omega = \frac{1}{\int \Phi_{ref,ref}(\bar{\omega})d\bar{\omega}}\int_{\omega-\Delta\omega}^{\omega+\Delta\omega} \mathcal{E}^2(\omega)d\omega = \int_{\omega-\Delta\omega}^{\omega+\Delta\omega} \frac{\mathcal{E}^2(\omega)}{\int \Phi_{ref,ref}(\bar{\omega})d\bar{\omega}}d\omega \tag{16}$$

The square-root of the resulting values indicate the percentage of the error that comes from the spectral band $\omega \pm \Delta\omega$ and the error contribution in relation to the signal standard deviation, for equation 15 and 16 respectively.

Frequency specific quality of an estimate The relative error estimate per frequency can be found by taking the limit of $\Delta\omega \to 0$ of the integral of the error spectrum and reference power spectrum:

$$\lim_{\Delta\omega\to 0} \frac{\int_{\omega-\Delta\omega}^{\omega+\Delta\omega} \mathcal{E}^2(\omega) d\omega}{\int_{\omega-\Delta\omega}^{\omega+\Delta\omega} \Phi_{ref,ref}(\bar{\omega}) d\bar{\omega}} \approx \frac{2\Delta\omega\mathcal{E}^2(\omega)}{2\Delta\omega\Phi_{ref,ref}(\omega)} = \frac{\mathcal{E}^2(\omega)}{\Phi_{ref,ref}(\omega)} \tag{17}$$

inserting equation 11 and 14 into equation 17, taking the square-root and rearranging we get the exact spectral equivalent of equation 1:

$$\frac{\mathcal{E}(\omega)}{\sqrt{\Phi_{ref,ref}(\omega)}} = \sqrt{1 + \frac{\sqrt{\Phi_{est,est}(\omega)}}{\sqrt{\Phi_{ref,ref}(\omega)}} \left(\frac{\sqrt{\Phi_{est,est}(\omega)}}{\sqrt{\Phi_{ref,ref}(\omega)}} - 2\mathcal{R}_{est,ref}(\omega) \right)}, \tag{18}$$

where the frequency specific relative error is a function of the frequency specific amplitude ratio between the estimate and reference signal and the frequency specific correlation coefficient.

4 Application to Experimental Pressure from PIV Data

Now that we have laid the foundation for going spectral and defined ways how to spectrally decompose the error, we will apply the decomposition to pressure from PIV data.

The data of de Kat and van Oudheusden (2012) is ideally suited, since it provides both pressure estimates from PIV as well as an independently measured reference signal from pressure transducers. The results for the overall error are included in 1 indicated by the lower two triangles. For the current analysis, we will assume that the reference signal is perfect and, therefore, any deviation from the reference signal is considered error. Using the power spectra and cross-power spectra we can determine the error power spectrum using equation 14.

Figure 2 shows the reference, estimated and error power spectra as well as the dynamic correlation for a pressure signal on the side of a square cylinder using stereo-PIV and the base of the cylinder using tomographic-PIV, the corresponding overall error $\sigma_{err}/\sigma_{ref}$ was about 20% and 75% respectively, see figure 1. The power spectrum of the pressure signal for the side of the square cylinder shows a clear peak at 20 Hz and a harmonic at 40 Hz; the estimated pressure spectrum follows the reference power spectrum closely up to 80 Hz above which the estimated pressure spectrum has higher values than the reference spectrum. The dynamic correlation shows values close to unity for low frequencies and drops to zero in the range 50–70 Hz. As one would expect, for the low frequencies, the error power spectrum is an order of magnitude smaller than the reference power spectrum, and, just like the estimate and reference power spectra, it peaks at 20 Hz. For frequencies above 80 Hz, the error power spectrum closely follows the estimated power spectrum.

The power spectrum of the pressure signal for the base of the square cylinder is much flatter in comparison with that of the side. It shows a peak at 40 Hz, with the estimate also having a peak at 20 Hz. The estimated pressure spectrum follows the reference power spectrum 200–300 Hz above which the estimated pressure spectrum flattens and remains at a higher value than the reference spectrum. The dynamic correlation shows that there is good correlation between the signals before it drops to zero around 200 Hz. For frequencies below, the error power is lower than the estimated and reference spectrum, except for 20 Hz. At 20 Hz there is an increase in the error spectrum, because the estimated and reference power spectra differ significantly and the dynamic correlation also shows a dip. Above 300 Hz, the error power spectrum closely follows the estimated power spectrum as was the case for the side pressure.

The error power spectrum will now be looked at in the different ways defined in the previous section. We will express the error power spectrum as contributions to the total error variance as fractions of σ^2_{err} and as fractions of σ^2_{ref}, and provide the results for the spectral equivalent of equation 1.

Figure 3 shows the fractional contributions of the error power spectrum to the error variance and the result of applying equation 18. The fractional contributions to the error variance (top) show that for both cases there is one main contributing frequency, 20 Hz, which accounts for about 50% and 20% of the error variance for the side and base (*left* and *right*) respectively. For the side pressure signal, this is also the frequency where the signal has its peak power content, see figure 2 *left*.

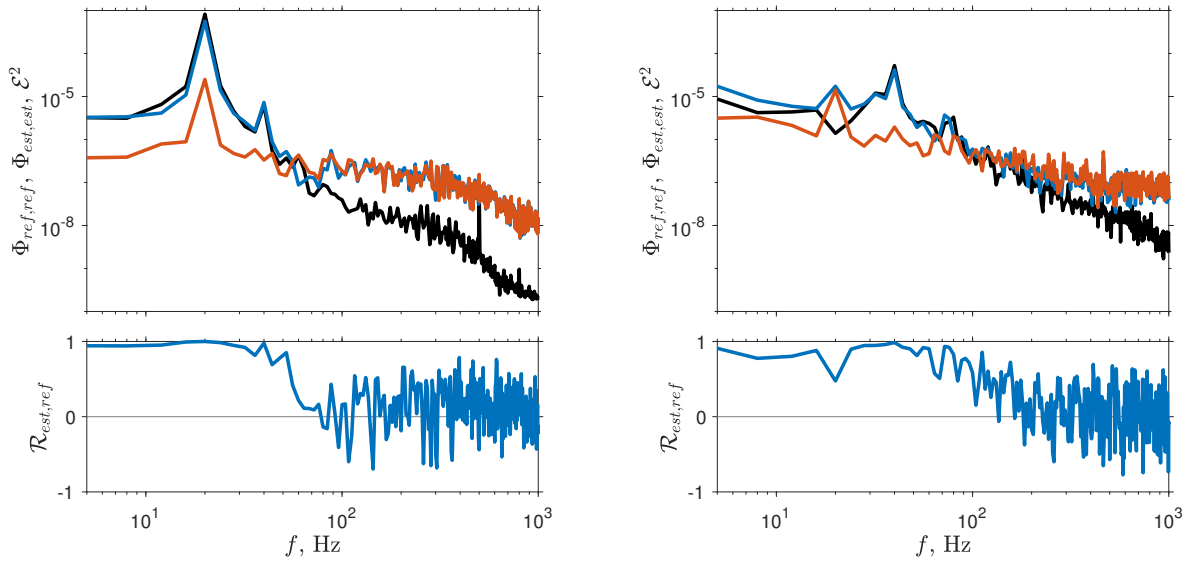

Figure 2: Estimated, reference and error power spectra and dynamic correlation for wall pressure on a square cylinder indicate how well the frequency content of the pressure signals is captured. Estimate, reference power spectra and dynamic correlation from de Kat and van Oudheusden (2012), error power spectrum from equation 14. *Top:* Estimated, reference and power spectra. Comparing the estimated power spectrum (*blue* line) with the reference power spectrum (*black* line) indicates how well the variance (or amplitude) is captured at each frequency. However, the error power spectrum (*red* line) is the result of both amplitude and phase differences. *Bottom:* Dynamic correlation is a frequency specific cross-correlation that indicates the phase match between the estimate and reference signals. *Left:* Side wall pressure results. *Right:* Base wall pressure results.

Interestingly, the results of applying equation 18 indicate that the frequency that contributes most to the error variance is actually the frequency that is best described, ie has the lowest frequency specific error (figure 3 *bottom–left*). This can be explained by the fact that 20 Hz has the highest power content for the side wall pressure signal and therefore, even if we only make a small error (compared to the other frequencies) of that power content, it can still be the largest contribution to the total error. The results for the base pressure signal shows that the frequency that contributes most to the total error is also poorly described, as one could also see from the power spectra and the dynamic correlation.

5 Discussion

Now that we have tools to decompose the error into its spectral contributions and have shown their application to experimental data, we will discuss briefly how they can be used.

Previous studies have used power spectra in combination with dynamic correlation (de Kat and van Oudheusden, 2012) or the modulus of the coherency (Ghaemi et al., 2012; Schneiders et al., 2016, who call it 'coherence' in their work) to show the quality of pressure from PIV compared with reference wall pressure measurement by pressure transducer or microphone, respectively. From the current work it follows that the dynamic correlation in combination with the power spectra allows one to determine the error power spectrum (with its integral being the error variance). In fact, the dynamic correlation can be seen as a per frequency cross-correlation and therefore is a measure for whether two signals match in phase. The modulus of coherency (or the coherence) does not distinguish in phase and therefore is a measure for how well signals *could* match is phase were perfectly corrected and will therefore over-predict the quality of an estimate. Therefore, we would propose that for quantifying the performance of a signal one should use the power spectra in combination with the dynamic correlation and ideally also include the error power spectrum (which can be easily obtained from them).

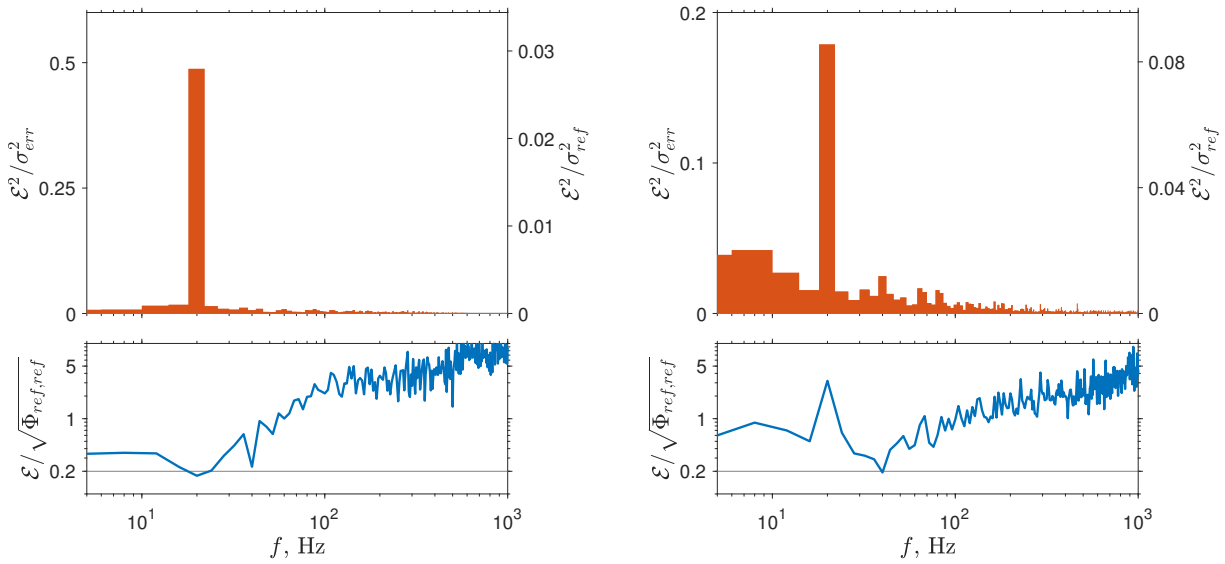

Figure 3: Spectral decomposition of RMSe shows how each frequency contributes to the error variance and how well each frequency is captured individually. *Top:* Fractional contributions to the error variance. *Bottom:* Frequency specific error. *Left:* Side wall pressure results. *Right:* Base wall pressure results.

The error power spectrum can be normalised with the error variance (or the signal variance) to show the fractional contribution to the error to identify dominant frequencies. When the main contributors are different from the frequencies of interest, temporal/spectral filtering could improve the estimate and reduce the error in the signal. When the main contributing frequency is the frequency of interest, little improvement is (likely) possible. For single point probes, one could determine a transfer function to correct the spectral content, but since the pressure from PIV estimate / PIV estimates depend on a field measurement, a correction is ill-posed and one would need to resort to ways to assimilate the correction for one point in the complete domain.

The final measure introduced in this work is the frequency specific error estimate. This estimate is of particular interest in its potential for estimating errors (uncertainty) for difficult cases, where reference measurements are unfeasible. For these cases, one could set up their pressure from PIV system, test the system on a reference case which includes are reference measurement and determine the frequency specific error. Then replacing the reference model with the model that need to be tested, one can use the frequency specific error and the estimated power spectrum by multiplying the two (after squaring the frequency specific error) to obtain an estimate of the error power spectrum – and hence the error on the pressure fluctuations. For this approach to work, one would need to do careful tests to identify whether the error is caused by systematic offsets (eg gain errors) or random deviations (system random noise). This would require spectrally full signals of various strengths. Ideally, such an investigation would allow us to find the driving parameters that result in errors and create a detailed model to predict the accuracy of the pressure from PIV estimates, without performing extensive reference measurements. The theoretical underpinnings for such models are currently under consideration.

6 Conclusion

In this work, we have laid the mathematical foundation to decompose the root-mean-square error of the estimate of pressure from PIV in its spectral constituents and shown their application to experimental estimates against reference signals. The error power spectrum was found to be the result of both amplitude and phase errors, where the phase errors correctly captured in the co-spectrum. The modulus of coherency or the coherence (as used in different studies) disregard phase errors and therefore overestimate the quality of an estimate and are more suited to indicate how good the estimate *could* predict the reference, iff phase

were to be perfectly corrected. Dominant contributing frequencies can be the best described frequencies, in which case little reduction of the error is likely possible. Frequency specific errors were defined and, for cases where obtaining a reference signal is unfeasible, their potential application to estimate errors were discussed.

Acknowledgements

This work is supported by EU-H2020 project HOMER (Grant agreement no. 769237). The author would like to acknowledge Dr Alexander Wittig for his knowledgable support in going spectral and decomposition.

References

Bendat JS and Piersol AG (2010) *Random Data*. Wiley

Croux C, Forni M, and Reichlin L (2001) A measure of comovement for economic variables: Theory and empirics. *The Review of Economics and Statistics* 83:232–241

de Kat R and van Oudheusden BW (2012) Instantaneous planar pressure determination from PIV in turbulent flow. *Experiments in Fluids* 52:1089–1106

Ghaemi S, Ragni D, and Scarano F (2012) PIV-based pressure fluctuations in the turbulent boundary layer. *Experiments in Fluids* 53:1823–1840

Liu X and Katz J (2006) Instantaneous pressure and material acceleration measurements using a four-exposure PIV system. *Experiments in Fluids* 41:227–240

McClure J and Yarusevych S (2017) Optimization of planar PIV-based pressure estimates in laminar and turbulent wakes. *Experiments in Fluids* 58:62

Schneiders JFG, Pröbsting S, Dwight RP, van Oudheusden BW, and Scarano F (2016) Pressure estimation from single-snapshot tomographic PIV in a turbulent boundary layer. *Experiments in Fluids* 57:53

Van der Kindere J, Laskari A, Ganapathisubramani B, and de Kat R (2019) Pressure from snapshot 2D PIV. *Experiments in Fluids* 60:32

van Gent P, Michaelis D, van Oudheusden B, Weiss PE, de Kat R, Laskari A, Jeon Y, David L, Schanz D, Huhn F, Gesemann S, Novara M, McPhaden C, Neeteson N, Rival D, Schneiders J, and Schrijer F (2017) Comparative assessment of pressure field reconstructions from particle image velocimetry measurements and Lagrangian particle tracking. *Experiments in Fluids* 58:33

van Oudheusden BW (2013) PIV-based pressure measurement. *Measurement Science and Technology* 24:032001